

## Understanding the One-Photon Photophysical Properties of a Two-Photon Absorbing Chromophore

Joy E. Rogers,<sup>\*,†,‡</sup> Jonathan E. Slagle,<sup>†,§</sup> Daniel G. McLean,<sup>†,⊥</sup> Richard L. Sutherland,<sup>†,⊥</sup> Bala Sankaran,<sup>†,||</sup> Ramamurthi Kannan,<sup>†,#</sup> Loon-Seng Tan,<sup>†</sup> and Paul A. Fleitz<sup>†</sup>

Materials and Manufacturing Directorate, Air Force Research Laboratory, 3005 Hobson Way, Bldg 651, Wright Patterson Air Force Base, Ohio 45433, UES, Inc., Dayton, Ohio 45432, AT&T Government Solutions, Dayton, Ohio 45324, Science Applications International Corporation, Dayton, Ohio 45434, Anteon Corporation, Dayton, Ohio 45431, and Systran Systems Corporation, Dayton, Ohio 45432

Received: March 8, 2004; In Final Form: April 30, 2004

A comprehensive one-photon photophysical study has been carried out on AF455, a known two-photon absorbing dye. AF455 is composed of an electron-accepting center with three arms that consist of a  $\pi$ -conjugated group with an electron-donating group at the terminal end of each arm. The objective of this work is to understand the one-photon excitation photophysical properties so that this knowledge will be carried into understanding the two-photon absorption properties. This was done by utilizing steady-state absorption, steady-state and time-resolved emission, femtosecond pump–probe, and nanosecond laser flash photolysis techniques. Through this study it was determined that AF455 undergoes an excited-state intramolecular charge transfer (ICT) upon absorption of a single photon. The extent of ICT stabilization is dependent on the solvent polarity, with increasing ICT stabilization in more polar solvents. The formation of the triplet excited state is small (<8%) and is effected only slightly by a change in the solvent polarity. With an increase in polarity the fluorescence quantum yield decreased and internal conversion was found to become more competitive. On the basis of a two-photon assisted excited-state absorption model we tied in the measured one-photon photophysical properties to understand why the nanosecond effective two-photon absorption cross section is much larger than the femtosecond intrinsic two-photon absorption cross section. We found that AF455 exhibits triplet excited-state absorption in the region of 800 nm that leads to enhancement of the nanosecond effective two-photon absorption cross section.

### Introduction

There has been much interest in the development of two-photon absorbing materials. A two-photon absorption process occurs when a material instantaneously absorbs two lower energy photons than needed for a linear absorption. These materials provide an advantage by exciting in the lower energy near-IR region resulting in the inherent higher energy photophysical properties of the chromophore. This is important to prevent damage to the material as a result of higher energy photons. There are a host of uses for two-photon absorbers that include use in optical data storage,<sup>1</sup> frequency upconverted lasing,<sup>2</sup> nonlinear photonics,<sup>3</sup> microfabrication,<sup>4</sup> fluorescence imaging,<sup>5</sup> and photodynamic therapy.<sup>6</sup> Significant advances in the design of these materials have been made recently but there is still some room for improvement.<sup>7,8</sup>

Specifically, a series of two-photon absorbing chromophores identified as AFX have been extensively studied.<sup>8</sup> These chromophores all contain a similar type geometry consisting of a D- $\pi$ -A (donor group– $\pi$ -conjugated group–acceptor group), A- $\pi$ -A, or D- $\pi$ -D geometry. Initially AF50 proved to be the best two-photon absorber when exciting at 800 nm with an ~8

ns laser pulse.<sup>8a</sup> As time went by attempts were made to modify the chromophores by changing the conjugated bridge and increasing the length of pendant side chains, as well as increasing the  $\pi$ -donor and acceptor strength.<sup>8b,i</sup> It was found that the addition of moderately long alkyl pendants to the fluorene bridging group not only imparts additional solubility but also increases the measured effective two-photon cross section. Improvements were also observed when changing the donor and acceptor groups. The series of chromophores have recently been expanded to include two- and three-arm chromophores that show improved two-photon absorption.<sup>8d,g,j,k,l</sup> To this date the materials that have the largest effective two-photon cross section, upon 800 nm nanosecond excitation, are AF450, AF455, and AF457.<sup>8l</sup> These chromophores consist of a 1,3,5-triazine electron-accepting center with three arms consisting of an electron-donating diphenylamino group and a dialkylfluorene aromatic bridge. The only difference is the pendant alkyl chain.

In addition to physical changes to the chromophore it has been shown that changes in the solvent polarity result in remarkably different effective two-photon cross sections.<sup>8a,f</sup> For AF50 a decrease in the nanosecond effective two-photon cross section with an increase in solvent polarity was observed.<sup>8a</sup> At the time no explanation was given for the differences in solvent. In 1999 a paper was published that specifically looks at the effects of the molecular environment on both linear and nonlinear properties.<sup>8f</sup> They found (1) that the stabilization of the linearly induced long-lived excited state by the local molecular environment can be predictably described with the

\* Address correspondence to this author. E-mail: joy.rogers@wpafb.af.mil.

† Wright Patterson Air Force Base.

‡ UES, Inc.

§ AT&T Government Solutions.

⊥ Science Applications International Corporation.

|| Anteon Corporation.

# Systran Systems Corporation.

Lippert equation, (2) that this understanding is applicable to the two-photon absorbing dyes and their excited-state absorption, and (3) that one-photon spectroscopic techniques offer a simple way to help establish structure–property relationships for effective two-photon behavior.

There have been many efforts made to understand why a material is a good two-photon absorber but it appears that this is still not well understood. We decided to pursue a more advanced study on one of the newer materials, AF455, to see how changing the solvent affects the overall one-photon photophysical properties and how these properties ultimately affect two-photon absorption. In the literature there are numerous cases where the intrinsic two-photon absorption cross section, measured with a femtosecond laser pulse, is several orders of magnitude smaller than the effective two-photon absorption cross section that is measured with a nanosecond laser pulse.<sup>7,8</sup> Because of the difference in cross-section measurements, transient species that live on the order of the laser pulse widths are important and need to be accounted for in a two-photon absorption process. It is suggested that the measured effective two-photon absorption cross section is characterized by a true two-photon absorption and a subsequent excited-state absorption.<sup>8c,9</sup> In this paper we map out the inherent one-photon photophysical properties of an AFX chromophore to show that the absorption spectra and kinetics of the various transient species are needed to understand the differences of two-photon absorption in the femtosecond and nanosecond time domains.

## Experimental Section

**Synthesis.** AF455 was prepared as previously described.<sup>81</sup>

**General Techniques.** Ground-state UV/vis absorption spectra were measured on a Cary 500 spectrophotometer. Emission spectra were measured on a Perkin-Elmer model LS 50B fluorometer. Nanosecond transient absorption measurements were carried out using the third harmonic (355 nm) of a Q-switched Nd:YAG laser (Quantel Brilliant, pulse width ca. 5 ns). Pulse fluences of up to 8 mJ cm<sup>-2</sup> at the excitation wavelength were typically used. A detailed description of the laser flash photolysis apparatus has been published earlier.<sup>10</sup>

Ultrafast transient absorption measurements were performed by using a modified version of the femtosecond pump–probe UV–vis spectrometer described elsewhere.<sup>11</sup> Briefly, 1-mJ, 100-fs pulses at 800 nm at a 1 kHz repetition rate were obtained from a diode-pumped, Ti:sapphire regenerative amplifier (Spectra Physics Hurricane). The output laser beam was split into pump and probe (85% and 15%) by a beam splitter. The pump beam was directed into a frequency doubler (CSK Super Tripler) and then was focused into the sample. The probe beam was delayed in a computer-controlled optical delay (Newport MM4000 250-mm linear positioning stage) and then focused into a sapphire plate to generate a white light continuum. The white light was then overlapped with the pump beam in a 2-mm quartz cuvette and then coupled into a CCD detector (Ocean Optics S2000 UV–vis). Data acquisition was controlled by software developed by Ultrafast Systems LLC.

Fluorescence quantum yields were determined by using the actinometry method previously described.<sup>10</sup> Quinine sulfate was used as an actinometer with a known fluorescence quantum yield of 0.55 in 1.0 N H<sub>2</sub>SO<sub>4</sub>.<sup>12</sup> All samples were excited at 340 nm with a matched optical density of 0.1.

Time-correlated single-photon counting (Edinburgh Instruments OB 920 Spectrometer) was utilized to determine singlet state lifetimes to fill in the region from the femtosecond transient absorption experiment (1.6 ns) cutoff to the nanosecond laser

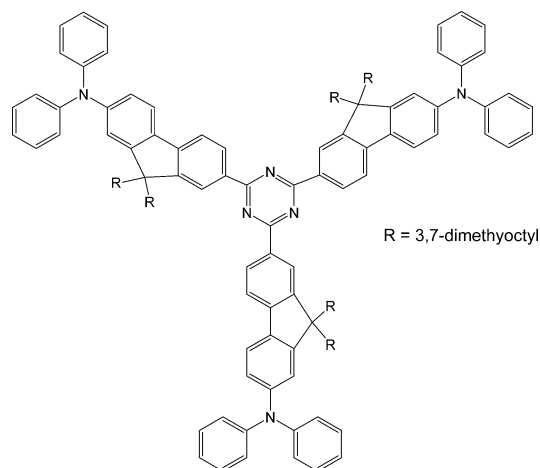


**Figure 1.** Chemical structure of electron donating– $\pi$ -electron accepting AF455.

flash photolysis experiments (100 ns). The sample was pumped with a 70-ps laser diode at 401 nm. Emission was detected on a cooled microchannel plate PMT. Data were analyzed by using a reconvolution software package provided by Edinburgh Instruments.

The molar absorption coefficient of the AF455 triplet state was determined by using the method of singlet depletion, which has been described previously.<sup>10</sup> Quantum yields for intersystem crossing were determined by using the method of relative actinometry as previously described utilizing a benzophenone actinometer.<sup>10</sup> Matched optical densities of AF455 and benzophenone at 355 nm were utilized in each determination.

## Results

**Ground-State Absorbance.** Shown in Figure 1 is the structure of AF455. It is composed of electron-donating diphenylamino groups, a dialkylfluorene aromatic bridge, and a 1,3,5-triazine electron-accepting group. Shown in Figure 2a are the ground state absorbance spectra of AF455 in various solvents. The spectral features are identical with that previously published in THF.<sup>81</sup> The various solvents were chosen because they represent increasing polarities and it is known in the literature that charge transfer absorbance bands are easily shifted with polarity,<sup>13</sup> where hexane is the most nonpolar and 2-propanol is the most polar based on their respective dielectric constants. With increasing polarity we observe a broadening of the spectrum. There appears to be no defined trend in the absorbance intensity (molar absorption coefficient) with increasing polarity.

**Fluorescence and Phosphorescence.** Shown in panel b of Figure 2 are the fluorescence spectra of AF455 in various air-saturated solvents. A significant red shift is observed with increasing polarity. This is typical behavior of chromophores that contain donor–acceptor moieties.<sup>13,14</sup> A similar phenomenon has been observed for other AFX chromophores.<sup>8a,f</sup> We also measured the fluorescence quantum yield of AF455 in each solvent under both air-saturated and deoxygenated conditions and found that it becomes smaller with increasing polarity. These values are given in Table 1 along with the maximum fluorescence peaks. The data in air-saturated THF agree fairly well with the fluorescence quantum yield previously found for AF455.<sup>81</sup> The phosphorescence spectra of AF455 in methylcyclohexane and methyltetrahydrofuran with 20% methyl iodide at 77 K are shown in Figure 2c. In the absence of methyl iodide we did not observe any phosphorescence from this material. Addition of methyl iodide to the methylcyclohexane solution

**TABLE 1: Summary of Photophysical Properties of AF455 in Various Solvents**

	hexane	benzene	THF	2-propanol
Dielectric constant	1.89	2.284	7.6	18.3
Abs <sub>max</sub>	418 nm	420 nm	414 nm	415 nm
FL <sub>max</sub>	432 nm	456 nm	496 nm	516 nm
Φ <sub>FL</sub> (air saturated)	0.75	0.67	0.42	0.25
Φ <sub>FL</sub> (deoxygenated)	0.90	0.70	0.43	0.24
Stokes shift	0.096 eV	0.231 eV	0.495 eV	0.585 eV
Ph <sub>max</sub>	546 nm <sup>a</sup>		554 nm <sup>b</sup>	
E <sub>T</sub>	2.30 eV		2.28 eV	
Φ <sub>ISC</sub> (air saturated)	0.075 ± 0.004	0.030 ± 0.002	0.060 ± 0.003	0.058 ± 0.003
Φ <sub>ISC</sub> (deoxygenated)	0.017 ± 0.001	0.017 ± 0.001	0.049 ± 0.002	0.050 ± 0.003

<sup>a</sup> Measured at 77 K in methylcyclohexane with 20% methyl iodide. <sup>b</sup> Measured at 77 K in methyltetrahydrofuran with 20% methyl iodide.

**TABLE 2: Excited-State Kinetics of AF455 in Various Solvents**

	hexane	benzene	THF	2-propanol
τ <sub>1</sub> (air saturated)	0.30 ± 0.03 ps	0.45 ± 0.1 ps	1.66 ± 0.49 ps	2.03 ± 0.74 ps
τ <sub>2</sub> (air saturated)	2.2 ± 0.6 ps	3.8 ± 2.2 ps	48.6 ± 29.3 ps	36.4 ± 10.1 ps
τ <sub>3</sub> (air saturated)	1.256 ± 0.023 ns	1.477 ± 0.047 ns	2.718 ± 0.117 ns	2.634 ± 0.053 ns
τ <sub>4</sub> (air saturated)	106 ± 15 ns	142 ± 25 ns	368 ± 104 ns	196 ± 143 ns
τ <sub>4</sub> (deoxygenated)	135 ± 47 μs	219 ± 45 μs	53 ± 10 μs	42 ± 10 μs
τ <sub>5</sub> (deoxygenated)	> 1 ms	> 1 ms	~410 μs	~225 μs

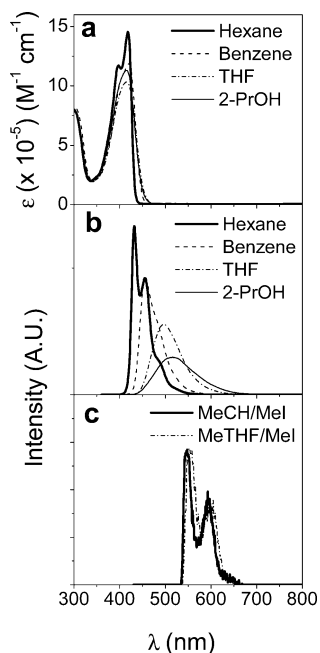


**Figure 2.** Shown in the top panel (a) are the ground state absorbance spectra of AF455 in hexane, benzene, THF, and 2-propanol. For benzene, THF, and 2-propanol the spectra are nearly identical. Panel b shows the fluorescence spectra in these same solvents. Samples were excited at 340 nm with a matched OD of 0.1. Shown in panel c are the phosphorescence spectra (normalized) in methyl cyclohexane or methyl tetrahydrofuran. Methyl iodide (20%) was added to each. Samples were excited at the absorbance peak maximum (415 nm). All data were obtained in air-saturated solvent at room temperature (25 °C) except for the phosphorescence, which was obtained at 77 K.

caused a shift in the observed fluorescence spectrum, indicating a change in the solvent environment. The methyl tetrahydrofuran with added methyl iodide has the same properties as THF, indicating that the overall solvent environment is similar. The phosphorescence maximum is given in Table 1 for both solvents. A small red shift was observed in the phosphorescence with increasing polarity.

**S<sub>1</sub>–S<sub>n</sub> Properties.** Figure 3 shows the ultrafast transient absorption spectra of AF455 in the four air-saturated solvents upon excitation with a 100-fs 400-nm pulse. For all solvents a multiexponential decay was found. Initially a very fast transient

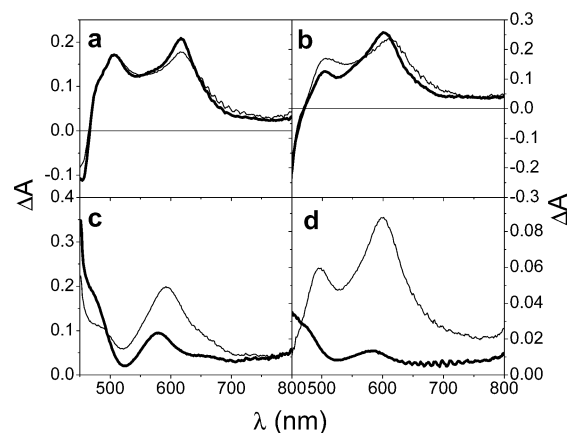


**Figure 3.** Shown are femtosecond transient absorption spectra of AF455 in (a) hexane (41.5 μM), (b) benzene (53.9 μM), (c) THF (67.9 μM), and (d) 2-propanol (38.3 μM) upon 400-nm excitation. Two times are shown, ~2 ps (lighter line) and around 50 ps (darker line) after the 100 fs laser pulse.

state was observed that decays within 2 ps in all solvents. These data are given in Table 2 as τ<sub>1</sub>. A second species (τ<sub>2</sub>) was found to live on the order of 2–49 ps depending on the solvent. At approximately 2 ps after the laser pulse a transient absorption was observed with a maximum at 617 (hexane), 610 (benzene), 593 (THF), and 600 nm (2-propanol). This is shown in Figure 3. In hexane the transient state grows (τ = 2.2 ps) with very little shift into a new transient state with an absorption maximum also at 617 nm. For benzene we observed a transient absorption that also grows in (τ = 3.8 ps) but is shifted to 602 nm, indicating the formation of a new transient state. The transient state formed for THF decays with a lifetime of 48.6 ps with a shift from 593 to 578 nm. Concomitant with the decay at 593 nm is a growth of a new transient absorption in the region from 450 to 500 nm. For 2-propanol the transient absorption at 600 nm decays with a lifetime of 36.4 ps to a new transient state with a maximum peak at 585 nm. Also concomitant with this decay is a growth around 450 nm. The multiple lifetimes are consistent with data obtained for AF50 and AF250.<sup>8c</sup>

**Time-Resolved Fluorescence.** To look at longer times than the femtosecond experiment allowed, time-correlated single-photon counting was done. Single-exponential fluorescence decays were measured for each solvent. These are given as τ<sub>3</sub>

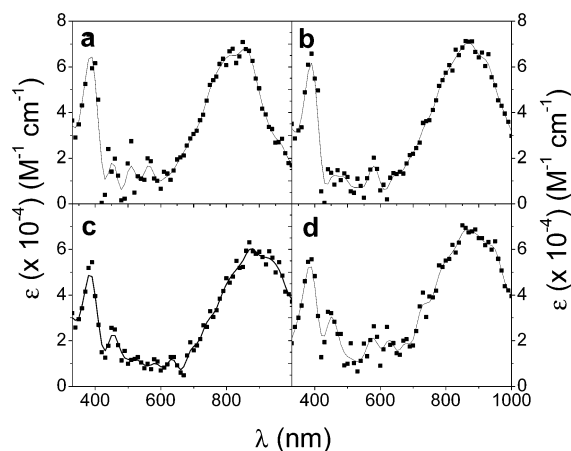


**Figure 4.**  $T_1-T_n$  absorption spectra observed after nanosecond pulsed 355-nm excitation of AF455 in (a) hexane (8.3  $\mu\text{M}$ ), (b) benzene (8.8  $\mu\text{M}$ ), (c) THF (9.2  $\mu\text{M}$ ), and (d) 2-propanol (8.5  $\mu\text{M}$ ). Samples were deoxygenated by the freeze-pump-thaw method. Molar absorption coefficients were obtained by using the method of singlet depletion.

in Table 2 for each solvent. With an increase in the polarity of the solvent the observed lifetime becomes longer ( $\tau_3$ ). For 2-propanol the lifetime is actually shorter than THF. The differences are due to aprotic versus protic solvent effects. In hindsight 2-propanol was probably not the best choice for this series of solvents because of its protic nature.

**$T_1-T_n$  Properties.** Shown in Figure 4 are the transient spectra obtained upon 355-nm excitation of AF455 in deoxygenated hexane, benzene, THF, and 2-propanol. A small shift in the peak maximum was observed with increasing polarity. The identities of the transients were confirmed by molecular oxygen quenching of the excited state and also by energy transfer sensitization to  $\beta$ -carotene. The  $T_1-T_n$  molar absorption coefficients were determined with a singlet depletion method. The intensity of the peak maximum is very similar in all solvents (hexane  $\epsilon_{850 \text{ nm}} = 67\,500 \pm 3\,400 \text{ M}^{-1} \text{ cm}^{-1}$ ; benzene  $\epsilon_{870 \text{ nm}} = 70\,700 \pm 3\,500 \text{ M}^{-1} \text{ cm}^{-1}$ ; THF  $\epsilon_{880 \text{ nm}} = 60\,000 \pm 3\,000 \text{ M}^{-1} \text{ cm}^{-1}$ ; 2-propanol  $\epsilon_{870 \text{ nm}} = 68\,700 \pm 3\,400 \text{ M}^{-1} \text{ cm}^{-1}$ ). Also given in Table 1 are the intersystem crossing quantum yields under both air-saturated and deoxygenated conditions. We observed that the yield is larger under air-saturated conditions. The opposite effect was observed in the fluorescence quantum yield where the yield became smaller in air-saturated solvent.

Shown in panel a of Figure 5 are the transient spectra of AF455 in deoxygenated 2-propanol at time zero and at 600  $\mu\text{s}$  following the laser pulse. The spectra have been normalized from 550 to 800 nm to highlight the differences in the bleaching region. Shown in the inset are the kinetic decays at 420 and 800 nm. It is evident from the kinetic data that a longer-lived species is present. The data at 600  $\mu\text{s}$  represent the spectral features of this long-lived transient as well as the still decaying triplet excited state. This is highlighted in the boxed area. The transient coincides very well with the ground-state absorption bleaching, which makes it difficult to discern an actual peak. The interesting thing about this long-lived transient is that the spectral features from 450 to 550 nm coincide with the growth at 450 nm in the femtosecond transient absorption data. This is shown in panel b of Figure 5 in THF. The data are normalized in the region from 450 to 550 nm to show the spectral similarities.

Under deoxygenated conditions the decay kinetics for THF are very similar to what was observed for 2-propanol and fit to a biexponential. For benzene and hexane the decays appear to

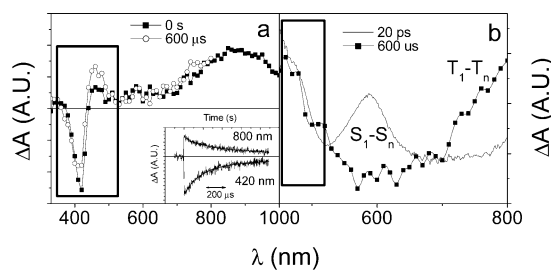
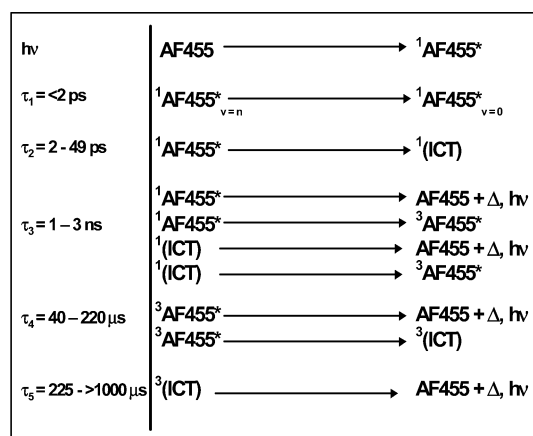


**Figure 5.** (a)  $T_1-T_n$  differential absorption spectra of AF455 (8.5  $\mu\text{M}$ ) in deoxygenated 2-propanol at time zero and 600  $\mu\text{s}$  after the laser pulse observed following nanosecond pulsed 355-nm excitation. The data at 600  $\mu\text{s}$  are normalized to overlay the time zero data in the region from 550 to 800 nm. Shown in the inset are the double exponential decays of the transient at 420 and 800 nm. (b) Overlaid femtosecond transient absorption data at 20 ps with nanosecond laser flash photolysis data at 600  $\mu\text{s}$  in THF. Data have been normalized in the 450–550 nm region to show spectral similarities in this region. The early time data are under air saturated conditions while the later data are under deoxygenated conditions.

### SCHEME 1: Various Pathways Depicting the Photophysical Processes of AF455



be single exponential but there is still a small absorptive long-lived tail that lives greater than 1 ms. Because the long-lived transient state does not relax on the time scale of our experiment the data were fit to a single exponential with a DC component. The kinetic data for all four solvents are given in Table 2. Under air-saturated conditions in all solvents no long-lived transient was observed. This points to a triplet-derived transient species that is noncompetitive with oxygen quenching.

### Discussion

The design and understanding of two-photon absorbing materials is very important to materials science because of their ability to absorb a lower energy wavelength to achieve the same results as that from a higher energy wavelength that is sometimes more destructive to the material. It is assumed that in the case of AF455 the one-photon absorption properties in the  $S_1$  level lead to the same photophysical behavior as in the two-photon (two photons with half the energy of the one photon) absorption case. On the basis of this assumption the one-photon photophysical processes (linear absorption) are discussed followed by a two-photon assisted excited-state absorption process (nonlinear absorption) that is based on the measured one-photon absorption properties.

**One-Photon Photophysical Processes.** Scheme 1 depicts the various pathways of deactivation upon absorption of a single photon. For AF455 in the various solvents up to a total of five

**TABLE 3: Rate Constants for Decay from the Singlet Excited State and/or ICT State**

	hexane	benzene	THF	2-propanol
$k_f(\text{air saturated})$	$6.0 \times 10^8 \text{ s}^{-1}$	$4.6 \times 10^8 \text{ s}^{-1}$	$1.6 \times 10^8 \text{ s}^{-1}$	$9.5 \times 10^7 \text{ s}^{-1}$
$k_{\text{ISC}}(\text{air saturated})$	$6.0 \times 10^7 \text{ s}^{-1}$	$2.0 \times 10^7 \text{ s}^{-1}$	$2.2 \times 10^7 \text{ s}^{-1}$	$2.2 \times 10^7 \text{ s}^{-1}$
$k_{\text{IC}}(\text{air saturated})$	$1.4 \times 10^8 \text{ s}^{-1}$	$2.0 \times 10^8 \text{ s}^{-1}$	$1.9 \times 10^8 \text{ s}^{-1}$	$2.6 \times 10^8 \text{ s}^{-1}$

lifetimes were observed under different conditions (air saturated vs deoxygenated). Upon absorption of energy the singlet excited state is formed within the 100-fs laser pulse. Within  $<2$  ps it is believed that the lowest vibrational level of the S1 state is fully occupied through intramolecular vibrational redistribution.<sup>15</sup> The intramolecular vibrational redistribution is internal conversion from higher energy levels (both vibrational and higher energy electronic states) to the lowest electronic state, the S1 manifold. This is shown in Scheme 1. With increasing polarity the vibrational relaxation takes longer in molecules having a more polar excited state because of increased solvent association around the state.

Depending on the polarity of the solvent (as determined by the dielectric constant) the S1 population relaxes to a new species proposed to be a solvent stabilized intramolecular charge transfer <sup>1</sup>(ICT) state derived from the singlet excited state (shown in Scheme 1). This is similar to 9,9'-bianthryl, *p*-(dimethylamino)benzonitrile, and 4-(*N,N*-dimethylamino)-4'-cyanobiphenyl, systems in the literature that form ICT states upon excitation.<sup>16</sup> For example, upon femtosecond excitation of 9,9'-bianthryl, a new transient species forms within 15–70 ps dependent on solvent, which is assigned to the solvent reorganized ICT state.<sup>16h</sup> Evidence for the formation of the singlet-derived solvent-stabilized <sup>1</sup>(ICT) state in AF455 is found in the femtosecond data shown in Figure 3. In THF and 2-propanol a new transient absorption grows in the region from 450 to 500 nm in the femtosecond data shown in Figure 3. The absorption due to the <sup>1</sup>(ICT) state is typically very similar energetically to the ground-state absorption but red shifted due to the lower energy of the <sup>1</sup>(ICT) state as confirmed by the large Stoke's shift in the fluorescence data (Table 1). Also, with increasing time a blue shift is observed in the overall transient spectrum for benzene, THF, and 2-propanol indicating formation of a new absorbing species. We observed no shift of the transient species in hexane indicating that very little to no solvent-stabilized <sup>1</sup>(ICT) state is formed. The formation time associated with this process becomes longer with polarity of the solvent indicating that the <sup>1</sup>(ICT) state for hexane is solvent stabilized much faster than in the case of 2-propanol.

Following solvent reorganization is competitive deactivation of both the S1 and <sup>1</sup>(ICT) states occurring by either internal conversion (IC) back to the ground state, fluorescence (fl), or intersystem crossing (ISC) to the triplet excited state. This is shown in Scheme 1. We observed that this lifetime becomes longer with increasing solvent polarity. Comparing the fluorescence quantum yields from Table 1 it is evident in less polar solvents that deactivation by fluorescence is the most predominant pathway. As the polarity of the solvent increased the fluorescence quantum yield decreased. However, no large increase was observed in the formation of the triplet excited state ( $\Phi_{\text{ISC}}$ ).

To understand the origin of the decrease in the fluorescence quantum yield the rate constants for decay from the singlet excited state and/or solvent stabilized <sup>1</sup>(ICT) state are given in Table 3. With increasing polarity an overall increase in internal conversion is observed becoming the dominate pathway of deactivation. The question that remains in this system is whether fluorescence, intersystem crossing, and internal conversion occur from the singlet manifold or the solvent-stabilized <sup>1</sup>(ICT) state

or a mixture of both. We know that the fluorescence is occurring from predominately the S<sub>1</sub> state in hexane because of good overlap of the ground-state absorption (S<sub>0</sub>–S<sub>1</sub>) and fluorescence spectra (S<sub>1</sub>–S<sub>0</sub>). In the other solvents we believe that emission is occurring from both the S<sub>1</sub> and <sup>1</sup>(ICT) state based on the shift and spectral features of the fluorescence data shown in Figure 2. The same is true for internal conversion and intersystem crossing. Looking at Table 3, clearly increasing the amount of solvent-stabilized <sup>1</sup>(ICT) state formed results in more efficient internal conversion rather than a large increase in intersystem crossing as has been found in other ICT systems.<sup>16e</sup>

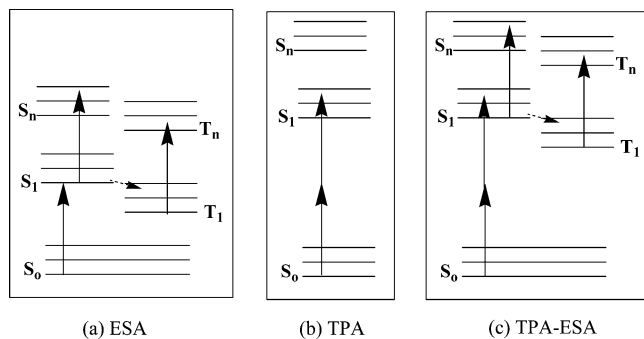
We observed that in the presence of oxygen the intersystem crossing quantum yield increases and the fluorescence quantum yield decreases as shown in Table 1. There are several possible explanations due to the paramagnetic properties of oxygen for the observed increase in intersystem crossing that has recently been reviewed in the literature in detail.<sup>17</sup> One example is a direct quenching of the AF455 singlet excited state resulting in the formation of the AF455 triplet excited state and ground-state molecular oxygen (<sup>3</sup>Σ<sub>g</sub><sup>-</sup>). A second example is the formation of the AF455 triplet excited state through excited singlet state quenching by molecular oxygen leading to the production of singlet oxygen (<sup>1</sup>Δ<sub>g</sub>). The singlet–triplet energy gap (S<sub>1</sub>–T<sub>1</sub>) of AF455 is much smaller than needed to produce singlet oxygen (<sup>1</sup>Δ<sub>g</sub>) (94 kJ/mol) so therefore we can rule out this mechanism and assume that the increase in intersystem crossing quantum yield is mainly due to the first quenching process. The differences in the intersystem crossing quantum yields are not consistent due to different concentrations of oxygen dissolved in the solvent with hexane being the largest (3.1 mM) followed by 2-propanol (2.2 mM), THF (2.1 mM), and benzene (1.9 mM).<sup>18</sup>

By using nanosecond laser flash photolysis we were able to identify the triplet excited state. Under air-saturated conditions the nanosecond resolved transient decayed with a single-exponential decay giving the lifetimes shown in Table 2. For the aprotic solvents the lifetime becomes longer with increasing polarity. The lifetime in 2-propanol is shorter than THF due to interaction with the solute.

Under deoxygenated conditions the kinetics observed are biexponential. We believe that  $\tau_4$  is due to decay of the triplet excited state concomitant with formation of a triplet-derived solvent-stabilized <sup>3</sup>(ICT) state. This is shown in Figure 5b where a transient is observed to grow in the same 450–550 nm region as that found in the femtosecond data. At the short 20-ps time scale the solvent-stabilized <sup>1</sup>(ICT) state is derived from a singlet state where in the case of the 600-μs data we believe the solvent-stabilized <sup>3</sup>(ICT) state is derived from a triplet excited state. Unfortunately in both cases we are unable to resolve the <sup>1,3</sup>(ICT) absorption spectrum because of overlaying S<sub>0</sub>–S<sub>1</sub> absorption. Furthermore, the kinetic behavior of the triplet excited state follows that of the singlet excited state where in both THF and 2-propanol the intensity of the transient formed in the 450–550 nm region is more than that in hexane and benzene where there is less <sup>1,3</sup>(ICT) solvent stabilization.

The triplet-derived solvent-stabilized <sup>3</sup>(ICT) state formed under deoxygenated conditions was found to decay on the order of 225 to  $>1000$  μs. The exact lifetime of decay of this species is difficult to measure because of limitations by the laser flash

**SCHEME 2: Comparison of (a) Excited-State Absorption, (b) Two-Photon Absorption, and (c) Two-Photon Assisted Excited-State Absorption.**



photolysis method. In THF and 2-propanol the data were fit to a biexponential decay and the lifetimes for  $\tau_5$  shown in Table 2 were obtained. These are estimates but it is clear that this species when formed lives for a significant time. In both hexane and benzene a long-lived transient was observed but we were unable to determine a reliable biexponential fit. We estimate the lifetimes to be longer than 1 ms.

Overall we have been able to map out the spectral and kinetic properties of AF455 in various solvents. We did find that the kinetic properties do not include simple deactivation from a singlet excited state or triplet excited state but rather a competition from these states with a solvent-stabilized  $^{1,3}$ (ICT) state. On the basis of these properties we will now apply this to the two-photon absorption properties.

**Two-Photon-Assisted Excited-State Absorption.** As mentioned previously there have been many efforts made to understand why a material is a good two-photon absorber but it appears that this is still not well understood. In the literature it is suggested that the measured effective two-photon absorption cross section with a nanosecond laser pulse is characterized by a true two-photon absorption and a subsequent excited-state absorption.<sup>8c,9</sup> To understand the concept of this we have illustrated the mechanism of a two-photon-assisted excited-state absorption in Scheme 2. Shown are three models of absorption. The first (a) is a typical excited-state absorption using a five-level model (ESA). Upon absorption of a photon an electron is promoted to a higher singlet level, which then vibrationally relaxes back to the  $S_1$  level. A second photon is then absorbed either directly by an  $S_1-S_n$  transition or following intersystem crossing the photon is absorbed by the  $T_1-T_n$  transition. The second (b) model is a two-photon absorption (TPA) where it takes absorption of two photons of certain energy to reach the upper level singlet manifold. Finally, the third (c) model shows the two-photon-assisted excited-state absorption model (TPA-ESA). This model is based on (a) and (b) where two photons are needed to promote the electron to the singlet manifold and then a third photon is absorbed to either promote to higher  $S_n$  levels or following intersystem crossing to higher  $T_n$  levels. Equation one describes the intensity loss ( $I$ ) on propagation through the medium in a two-photon-assisted excited-state absorption model.<sup>9</sup>

$$\frac{\partial I}{\partial Z} = -\sigma_2 N^2 I^2 - \sigma_{ES} N_{ES} I \quad (1)$$

In this equation  $\sigma_2$  is the intrinsic two-photon absorbance cross section (determined through femtosecond measurements),  $\sigma_{ES}$  is the excited-state absorbance cross section,  $N$  is the number of molecules per unit volume, and  $N_{ES}$  is the number of excited-state molecules per unit volume.

For AF455 both the intrinsic two-photon absorption cross section  $\sigma_2$  (790 nm; measured with a fs pulse) and the effective two-photon absorption cross section (800 nm; measured with a ns pulse) have been measured in air-saturated THF to be  $0.51 \times 10^{-20} \text{ cm}^4/\text{GW}$  and  $134 \times 10^{-20} \text{ cm}^4/\text{GW}$ , respectively.<sup>81</sup> There is quite a substantial increase in the cross section under nanosecond irradiation. A theoretical model has recently been developed and explored in detail in our lab that correlates nanosecond nonlinear absorption data of AF455 with inherent photophysical properties.<sup>19,20</sup> Without detailing specifics of the model because it is being published elsewhere we propose that the mechanism for this enhanced nanosecond nonlinear two-photon absorption is in fact due to the excited-state absorption from the triplet excited state as shown in eq 1 and Scheme 2. The excited-state absorption in Scheme 2 is dependent on both  $S_1-S_n$  absorption and  $T_1-T_n$  absorption. Figure 3 shows that there is very little  $S_1-S_n$  absorption in the region of 790–800 nm, where the TPA measurements were previously made. However, in the  $T_1-T_n$  absorption data (Figure 4) the peak is centered close to the 790–800 nm region with variation due to solvent shifts. We believe that there is a significant enhancement in the nanosecond effective two-photon absorption cross section because of the triplet excited-state absorption in this region. On the basis of eq 1 it becomes apparent that the TPA-ESA process is dependent on kinetic processes because the number of excited-state molecules produced is dependent on the rate of intersystem crossing. One of the questions that will be addressed in more detail later is the effect of the various rates by solvent on the nonlinear absorption properties of AF455.<sup>20</sup>

## Conclusions

In this paper we present the one-photon photophysical properties and show that the solvent does change both the spectral properties and the kinetics. In general the formation of the solvent-stabilized intramolecular charge transfer (ICT) state was found to increase in more polar solvents. With increased solvent-stabilized ICT formation a decrease in fluorescence quantum yield was observed as well as a red shift in the overall fluorescence spectrum. Intersystem crossing is only affected slightly by increased solvent-stabilized ICT formation, most likely because of its small inherent quantum yield (<8%).

On the basis of a two-photon-assisted excited-state absorption model we tie in the measured one-photon photophysical properties to understand why the nanosecond effective two-photon absorption cross section is much larger than the femtosecond intrinsic two-photon absorption cross section. We have shown that AF455 does have a triplet excited-state absorption in the region of 800 nm that enhances the effective two-photon absorption cross section.

**Acknowledgment.** We are thankful for the support of this work by AFRL/ML Contracts F33615-99-C-5415 for D.G.M. and R.L.S., F33615-03-D-5408 for B.S., F33615-94-C-5804 for R.K., and F33615-03-D-5421 for J.E.R. and J.E.S. and the Air Force Office of Scientific Research (AFOSR). We thank Evgeny Danilov and Prof. Michael Rodgers for use of the femtosecond transient absorption experiment at the Ohio Laboratory for Kinetic Spectrometry located at Bowling Green State University.

## References and Notes

- (1) (a) Parthenopoulos, D. A.; Rentzepis, P. M. *Science* **1989**, *249*, 843. (b) Dvornikov, A. S.; Rentzepis, P. M. *Opt. Commun.* **1995**, *119*, 341.
- (2) (a) Bhawalkar, J. D.; He, G. S.; Prasad, P. N. *Rep. Prog. Phys.* **1996**, *59*, 1041. (b) He, G. S.; Zhao, C. F.; Bhawalkar, J. D.; Prasad, P. N.

- Appl. Phys. Lett.* **1995**, *78*, 3703. (c) Zhao, C. F.; He, G. S.; Bhawalkar, J. D.; Park, C. K.; Prasad, P. N. *Chem. Mater.* **1995**, *7*, 1979.
- (3) (a) Fleitz, P. A.; Sutherland, R. A.; Ananthavel, S. P.; Larson, F. P.; Dalton, L. R. *SPIE Proc.* **1998**, *3472*, 91. (b) He, G. S.; Bhawalkar, J. D.; Zhao, C. F.; Prasad, P. N. *Appl. Phys. Lett.* **1995**, *67*, 2433. (c) Ehrlich, J. E.; Wu, X. L.; Lee, L. Y.; Hu, Z. Y.; Roeckel, H.; Marder, S. R.; Perry, J. *Opt. Lett.* **1997**, *22*, 1843.
- (4) (a) Kawata, S.; Sun, H. B.; Tanaka, T.; Takada, K. *Nature* **2001**, *412*, 697–698. (b) Cumpston, B. H.; Ananthavel, S. P.; Barlow, S.; Dyer, D. L.; Ehrlich, J. E.; Erskine, L. L.; Heikal, A. A.; Kuebler, S. M.; Le, I. Y. S.; McCord-Maughon, D.; Qin, J.; Rockel, H.; Rumi, M.; Wu, X. L.; Marder, S. R.; Perry, J. W. *Nature* **1999**, *398*, 51.
- (5) Denk, W.; Strickler, J. H.; Webb, W. W. *Science* **1990**, *248*, 73.
- (6) Bhawalkar, J. D.; Kumar, N. D.; Zhao, C. F.; Prasad, P. N. *J. Clin. Laser Med. Surg.* **1997**, *15*, 201.
- (7) (a) Prasad, P. N.; Reinhardt, B. A. *Chem. Mater.* **1990**, *2*, 660. (b) Zhao, M.; Samoc, M.; Prasad, P. N.; Reinhardt, B. A.; Unroe, M. R.; Prazak, M.; Evers, R. C. Kane, J. J.; Jariwala, C.; Sinsky, M. *Chem. Mater.* **1990**, *2*, 670. (c) Pan, H.; Gao, X.; Zhang, Y.; Prasad, P. N.; Reinhardt, B.; Kannan, R. *Chem. Mater.* **1995**, *7*, 816. (d) He, G. S.; Gvishi, R.; Prasad, P. N.; Reinhardt, B. A. *Opt. Commun.* **1995**, *117*, 133. (e) He, G. S.; Xu, G. C.; Prasad, P. N.; Reinhardt, B. A.; Bhatt, J. C.; Dillard, A. G. *Opt. Lett.* **1995**, *20*, 435. (f) He, G. S.; Bhawalkar, J. D.; Prasad, P. N.; Reinhardt, B. A. *Opt. Lett.* **1995**, *20*, 1524. (g) Larson, E. J.; Friesen, L. A.; Johnson, C. K. *Chem. Phys. Lett.* **1997**, *265*, 161. (h) Chung, S. J.; Kim, K. S.; Lin, T. C.; He, G. S.; Swiatkiewicz, J.; Prasad, P. N. *J. Phys. Chem. B* **1999**, *103*, 10741–10745. (i) Oberle, J.; Bramerie, L.; Jonusauskas, G.; Rulliere, C. *Opt. Commun.* **1999**, *169*, 325. (j) Kotler, Z.; Segal, J.; Sigalov, M.; Ben-Asuly, A.; Khodorkovsky, V. *Synth. Met.* **2000**, *115*, 269. (k) Kim, O. K.; Lee, K. W.; Woo, H. Y.; Kim, K. S.; He, G. S.; Swiatkiewicz, J.; Prasad, P. N. *Chem. Mater.* **2000**, *12*, 284. (l) Adronov, A.; Frechet, J. M. J.; He, G. S.; Kim, K. S.; Chung, S. J.; Swiatkiewicz, J.; Prasad, P. N. *Chem. Mater.* **2000**, *12*, 2838. (m) Belfield, K. D.; Bondar, M. V.; Przhonska, O. V.; Schafer, K. J.; Mourad, W. J. *Luminescence* **2002**, *97*, 141. (n) Patra, A.; Pan, M.; Friend, C. S.; Lin, T. C.; Cartwright, A. N.; Prasad, P. N.; Burzynski, R. *Chem. Mater.* **2002**, *14*, 4044–4048. (o) Martineau, C.; Lemercier, G.; Andraud, C. *Opt. Mater.* **2002**, *21*, 555. (p) Meng, F.; Mi, J.; Qian, S.; Chen, K.; Tian, H. *Polymer* **2003**, *44*, 6851. (q) Mongin, O.; Brunel, J.; Porres, L.; Blanchard-Desce, M. *Tetrahedron Lett.* **2003**, *44*, 2813. (r) Mongin, O.; Porres, L.; Katan, C.; Pons, T.; Mertz, J.; Blanchard-Desce, M. *Tetrahedron Lett.* **2003**, *44*, 8121. (s) Brousriche, D. W.; Serin, J. M.; Frechet, J. M. J.; He, G. S.; Lin, T. C.; Chung, S. J.; Prasad, P. J. *Am. Chem. Soc.* **2003**, *125*, 1448.
- (8) (a) He, G. S.; Yuan, L.; Cheng, N.; Bhawalkar, J. D.; Prasad, P. N.; Brott, L. L.; Clarkson, S. J.; Reinhardt, B. A. *J. Opt. Soc. Am. B* **1997**, *14*, 1079. (b) Reinhardt, B. A.; Brott, L. L.; Clarkson, S. J.; Dillard, A. G.; Bhatt, J. C.; Kannan, R.; Yuan, L.; He, G. S.; Prasad, P. N. *Chem. Mater.* **1998**, *10*, 1863. (c) Swiatkiewicz, J.; Prasad, P. N.; Reinhardt, B. A. *Opt. Commun.* **1998**, *157*, 135. (d) Joshi, M.; Swiatkiewicz, J.; Xu, F.; Prasad, P. N.; Reinhardt, B. A.; Kannan, R. *Opt. Lett.* **1998**, *23*, 1742. (e) Pudavar, H. E.; Joshi, M. P.; Prasad, P. N.; Reinhardt, B. A. *Appl. Phys. Lett.* **1999**, *74*, 1338. (f) Baur, J. W.; Alexander, M. D.; Banach, M.; Denny, L. R.; Reinhardt, B. A.; Vaia, R. A. *Chem. Mater.* **1999**, *11*, 2899. (g) He, G. S.; Swiatkiewicz, J.; Jiang, Y.; Prasad, P. N.; Reinhardt, B. A.; Tan, L. S.; Kannan, R. *J. Phys. Chem. A* **2000**, *104*, 4805. (h) Sivaraman, R.; Clarkson, S. J.; Lee, B. K.; Steckl, A. J.; Reinhardt, B. A. *Appl. Phys. Lett.* **2000**, *77*, 328. (i) Kannan, R.; He, G. S.; Yuan, L.; Xu, F.; Prasad, P. N.; Dombroskie, A. G.; Reinhardt, B. A.; Baur, J. W.; Vaia, R. A.; Tan, L. S. *Chem. Mater.* **2001**, *13*, 1896. (j) He, G. S.; Lin, T. C.; Prasad, P. N.; Kannan, R.; Vaia, R. A.; Tan, L. S. *J. Phys. Chem. B* **2002**, *106*, 11081. (k) Chiang, L. Y.; Padmawar, P. A.; Canteenwala, T.; Tan, L. S.; He, G. S.; Kannan, R.; Vaia, R.; Lin, T. C.; Zheng, Q.; Prasad, P. N. *Chem. Commun.* **2002**, 1854. (l) Kannan, R.; He, G. S.; Lin, T. C.; Prasad, P. N.; Vaia, R. A.; Tan, L. S. *Chem. Mater.* **2004**, *16*, 185.
- (9) Sutherland, R. L. *Handbook of Nonlinear Optics*, 2nd ed., revised and expanded; Marcel-Dekker: New York, 2003.
- (10) Rogers, J. E.; Cooper, T. M.; Fleitz, P. A.; Glass, D. J.; McLean, D. G. *J. Phys. Chem. A* **2002**, *106*, 10108–10115.
- (11) Nikolaitchik, A. V.; Korth, O.; Rodgers, M. A. J. *J. Phys. Chem. A* **1999**, *103*, 7587.
- (12) Demas, J. N.; Crosby, G. A. *J. Phys. Chem.* **1971**, *75*, 991.
- (13) Valeur, B. *Molecular Fluorescence*; Wiley-VCH: Weinheim, Germany, 2002.
- (14) Lakowicz, J. R. *Principles of Fluorescence Spectroscopy*, 2nd ed.; Kluwer Academic/Plenum Publishers: New York, 1999.
- (15) Liu, J. Y.; Fan, W. H.; Han, K. L.; Deng, W. Q.; Xu, D. L.; Lou, N. Q. *J. Phys. Chem. A* **2003**, *107*, 10857.
- (16) (a) Wang, Y.; McAuliffe, M.; Novak, F.; Eisenthal, K. B. *J. Phys. Chem.* **1981**, *85*, 3736. (b) Anthon, D. W.; Clark, J. H. *J. Phys. Chem.* **1987**, *91*, 3530. (c) Kang, T. J.; Kahlow, M. A.; Giser, D.; Swallen, S.; Nagarajan, V.; Jarzeba, W.; Barbara, P. F. *J. Phys. Chem.* **1988**, *92*, 6800. (d) Mataga, N.; Yao, H.; Okada, T.; Rettig, W. *J. Phys. Chem.* **1989**, *93*, 3383–3386. (e) Schutz, M.; Schmidt, R. *J. Phys. Chem.* **1996**, *100*, 2012. (f) Maus, M.; Rettig, W. *Chem. Phys.* **1997**, *218*, 151. (g) Maus, M.; Rettig, W.; Bonafoux, D.; Lapouyade, R. *J. Phys. Chem. A* **1999**, *103*, 3388. (h) Jurczok, M.; Plaza, P.; Rettig, W.; Martin, M. M. *Chem. Phys.* **2000**, *256*, 137. (i) Kovalenko, S. A.; Perez Lustres, J. L.; Ernsting, N. P.; Rettig, W. *J. Phys. Chem. A* **2003**, *107*, 10228.
- (17) Schweitzer, C.; Schmidt, R. *Chem. Rev.* **2003**, *103*, 1685.
- (18) Murov, S. L.; Carmichael, I.; Hug, G. L. *Handbook of Photochemistry*, 2nd ed.; Marcel Dekker: New York, 1993.
- (19) Sutherland, R. L.; Brant, M. E.; McLean, D. G.; Rogers, J. E.; Sankaran, B.; Kirkpatrick, S. E.; Fleitz, P. A. *Proceedings from CLEO/QUELS*, 2004, manuscript submitted.
- (20) Sutherland, R. L.; Brant, M.; Rogers, J. E.; McLean, D. G.; Sankaran, B.; Kirkpatrick, S.; Fleitz, P. A. Manuscript in preparation.